Open access • Journal Article • DOI:10.1103/PHYSREVB.76.045319

Resonant polariton-polariton scattering in semiconductor microcavities

Michiel Wouters

Institutions: University of Antwerp

Published on: 17 Jul 2007 - Physical Review B (American Physical Society)

Topics: Polariton, Scattering, Exciton, Photon and Quantum well

Resonant polariton-polariton scattering in semiconductor microcavities

Michiel Wouters
TFVS, Universiteit Antwerpen, Groenenborgerlaan 171, 2020 Antwerpen, Belgium
(Received 9 January 2007; revised manuscript received 23 March 2007; published 17 July 2007)

We study the scattering of polaritons in a semiconductor microcavity in the strong-coupling regime between a quantum well exciton and a cavity photon. The scattering resonance due to the biexcitonic bound state is analyzed in detail. We point out its signatures in the parametric interaction strength, the mean-field shifts, and the orientation of the linear polarization of parametric luminescence.

DOI: 10.1103/PhysRevB.76.045319 PACS number(s): 71.36.+c, 72.20.Dp

I. INTRODUCTION

Scattering resonances play a prominent role in the manipulation of interactions in quantum many-body systems. In ultracold atomic gases, for example, magnetic Feshbach resonances[1,2] have been very successfully employed to tune the interactions between atoms and applied to observe a controlled collapse and subsequent explosion of a Bose-Einstein condensate[3] (BEC) as well as the BEC-BCS crossover in a two-component Fermi gas.[4]

Scattering in semiconductor microcavities in the strong-coupling regime between cavity photons and quantum well excitons has recently attracted a good deal of interest.[5] In the strong exciton photon coupling regime, the quasiparticles are polaritons, a coherent superposition of photon and exciton, from which the excitonic content is responsible for the interaction among the polaritons. In the channel of opposite circular polarization, the polaritons can form a bound state, the bipolariton, whose energy is close to the biexciton energy.[7] The first experimental evidence for the bipolariton was obtained by Saba *et al.*[6] in pump-probe reflection measurements. A more detailed theoretical and experimental analysis of the bipolariton in microcavities was reported in Ref. 8.

Because the biexciton binding energy is of the same order as the Rabi splitting between the upper and lower polariton branches, it is possible to tune the bipolariton energy close to the scattering continuum, in which case the polariton-polariton interactions are resonantly enhanced. Tartakovskii *et al.* have invoked this mechanism to explain their experimental observations.[9] They found that a linearly polarized pump gave rise to a stronger parametric emission as compared to a circularly polarized pump. The connection with the bipolariton is readily made, because only when both up and down circular polarizations of the polaritonic field are excited, the bipolaritonic state can play a role in the parametric scattering process. A quantitative theoretical treatment of polariton scattering close to the bipolariton has, however, not been performed yet. Moreover, in Ref. 10 it was argued that the bipolariton cannot play an important role in the polariton scattering, because it is mainly built up with high-momentum exciton states, whereas the parametric scattering experiments are carried out at low wave vectors.

It is the purpose of this paper to analyze the resonant polariton scattering in more detail within a contact interaction model for the exciton-exciton interaction, in the presence of both a biexcitonic state and strong light-matter coupling. We will only focus on the interactions between polaritons in the lower branch which is better protected from losses and calculate the nonlinear coupling constant—i.e., the prefactor of the nonlinear term in the Gross-Pitaevskii equation. It was pointed out by Kwong and co-workers that the optical nonlinearity is given by the T matrix,[11,12] which will be the primary quantity of interest in this paper.

We start in Sec. II with a model calculation of the excitonic T matrix and then generalize it to the polaritonic T matrix. In Sec. III, we discuss the consequences of the bipolaritonic scattering resonance on the parametric oscillation in microcavities, and in Sec. IV, we put forward other experimental signatures of the bipolaritonic scattering resonance, related to the change of sign of the coupling constant. This change of sign affects both the direction of the mean-field energy shifts and the orientation of linear polarization of parametric luminescence.

II. NONLINEAR COUPLING CONSTANT AND THE T MATRIX

If the interactions are sufficiently weak (to be quantified later), the dynamics of a resonantly pumped microcavity with strong coupling between a quantum well exciton and a cavity photon [effective two-dimensional (2D) system] can be described by a Gross-Pitaevskii equation for the lower polariton **C**-number fields $\psi_{LP,\sigma}$, which for a finite square of length L with periodic boundary conditions reads in Fourier space

$$i\hbar\frac{d}{dt}\psi_{LP\sigma}(\mathbf{k}) = \left[\varepsilon(\mathbf{k}) - i\frac{\gamma}{2}\right]\psi_{LP\sigma}(\mathbf{k}) + F_{p\sigma}(\mathbf{k})e^{-i\omega_p t} + \frac{1}{L^2}\sum_{K,q,\chi} g^{\sigma\chi}_{\mathbf{K},\mathbf{k},\mathbf{q}}\psi^*_{LP\chi}(\mathbf{K}-\mathbf{k})\psi_{LP\sigma}(\mathbf{K}-\mathbf{q})\psi_{LP\chi}(\mathbf{q}), \tag{1}$$

where $\varepsilon(\mathbf{k})$ and γ are, respectively, the lower polariton dispersion and lifetime. The second term represents the coherent driving by an external laser source with frequency ω_p whose wave vector and polarization profile is determined by $F_{p\sigma}(\mathbf{k})$. Interactions between polaritons are modeled by the last nonlinear term. The nonlinear coupling constant equals

$$g^{\sigma\chi}_{\mathbf{K},\mathbf{k},\mathbf{q}}(E) = L^{-2}\langle \mathbf{K}\mathbf{k};\sigma\chi|T_E|\mathbf{K}\mathbf{q}\sigma\chi\rangle, \tag{2}$$

where the T matrix is defined in terms of the interaction potential V and the full two-body Green function G_E as

$$T_E = V + VG_E V. \tag{3}$$

The ket $|\mathbf{Kq};\sigma\chi\rangle$ represents here a normalized two-particle state of momenta $\mathbf{q}$ and $\mathbf{K}-\mathbf{q}$ with spin projections on the growth axis σ and χ, respectively. The dependence of the interaction term in Eq. (1) on the spin degrees of freedom was simplified by using the rotational invariance of the microcavity and the s-wave exciton states.

In fact, low-energy scattering in two dimensions shows the peculiar behavior[13,14]

$$\langle 00|T_{E\to 0}|00\rangle = \frac{4\pi\hbar^2}{m[\ln(E_b/E) + i\pi]} \tag{4}$$

for particles with mass m, and for strictly zero scattering energy, the T matrix vanishes. In practice, however, this property does not often play an important role for the description of the many-body Bose gas. For example, in thermodynamical equilibrium, the many-body physics fixes the chemical potential $\mu = gn$ as the relevant energy scale and the correct way to obtain the coupling constant from the T matrix is to a first approximation[15]

$$g = \langle 00|T_{-\mu}|00\rangle, \tag{5}$$

where $\mu = gn$ has to be determined self-consistently. For sufficiently weak interactions, the exact value of μ substituted in the above formula is not crucial, because the chemical potential only enters in the logarithm and it is sufficient to put a number with the correct order of magnitude, at least as long as μ/E_b is not close to 1. Because $E=-E_b$ is a pole of the T matrix (4), there is a two-particle bound state at this energy. The condition $\mu \approx E_b$ implies that this bound state plays an important role in the many-body physics, a situation where mean-field theories typically fail and more complicated approaches have to be worked out (see, e.g., Ref. 16 for the 3D Bose gas with a low-lying bound state).

In general, the mean-field description (1) can only be used when the interaction energy is sufficiently weak with respect to the kinetic energy. The quantity to set a scale for the kinetic energy is the interparticle distance so that for a two-dimensional system of particles with mass m and density n the condition of weak interactions is $gn \ll \hbar^2 n/m$ or, equivalently, $g = 4\pi\hbar^2 t/m$ with dimensionless parameter $t \ll 1$.

A. Model

Strong coupling between the excitonic transition and the cavity photon in semiconductor microcavities is typically only achieved for wave vectors within a range of a few inverse microns around $k=0$: a polaritonic wave packet that is distorted on a length scale of less than 1 μm exits the strong-coupling regime. The excitonic interactions, on the other hand, take place on a much smaller length scale, roughly given by the inverse of the exciton radius, which is about 10 nm. This implies that for physics in the strong-coupling regime, the exciton-exciton interactions can be replaced by a zero-range contact interaction. Because we consider a two-dimensional system, such a contact interaction needs a proper regularization. For this purpose, we formulate the problem on a lattice and only let the lattice spacing a tend to infinity at the end of the calculations. In our model, the excitonic and photonic kinetic energies are modeled by a tunneling energy $t_{i,j}^{C,X}$ for hopping between sites i and j, chosen to reproduce the true dispersions of the cavity photons and excitons at long wavelengths $\lambda \gg a$.

Our model Hamiltonian reads then in terms of the cavity photon and exciton field operators ψ_C and ψ_X

$$H = \sum_{\mathbf{ij}} \sum_{\sigma} (\varepsilon^C \delta_{\mathbf{i,j}} + t_{\mathbf{i,j}}^C) \psi_{C\sigma}^\dagger(\mathbf{i}) \psi_{C\sigma}(\mathbf{j}) + \sum_{\mathbf{ij}} (\varepsilon^X \delta_{\mathbf{i,j}} + t_{\mathbf{i,j}}^X) \times \psi_{X\sigma}^\dagger(\mathbf{i}) \psi_{X\sigma}(\mathbf{j}) + \sum_{\mathbf{i}} \Omega_R [\psi_{C\sigma}^\dagger(\mathbf{i}) \psi_{X\sigma}(\mathbf{i}) + \psi_{X\sigma}^\dagger(\mathbf{i}) \psi_{C\sigma}(\mathbf{i})] + \sum_{\mathbf{i}\sigma\chi} \frac{g_0^{\sigma\chi}}{2} \psi_{X\sigma}^\dagger(\mathbf{i}) \psi_{X\chi}^\dagger(\mathbf{i}) \psi_{X\chi}(\mathbf{i}) \psi_{X\sigma}(\mathbf{i}). \tag{6}$$

We will consider the case of small detuning between cavity photonic level ε^C and the excitonic transition energy ε^X. The radiative and nonradiative loss processes as well as the longitudinal transverse splitting of the exciton polarization states[17] have been neglected, because they involve energy scales small as compared to the Rabi frequency Ω_R, so that the exciton-photon coupling is the major effect to renormalize the quasiparticle scattering.

B. Exciton-exciton scattering

Let us first consider a case without coupling between exctions and photons; i.e., we let the exciton-photon detuning be very large as compared to the Rabi frequency $|\varepsilon^C - \omega^X| \gg \Omega_R$, or equivalently we set $\Omega_R = 0$. The two-particle scattering problem is solved by calculating the T matrix (3). Its matrix elements between the two-particle states $|\mathbf{K},\mathbf{k}\rangle$ can be calculated by using the method presented in Ref. 18, yielding

$$\langle \mathbf{K},\mathbf{k};\sigma\chi|T_E^{XX}|\mathbf{K},\mathbf{k}';\sigma\chi\rangle_{XX} = \frac{L^2}{\frac{1}{g_0^{\sigma\chi}} - G_E^{Xo}(\mathbf{K})}, \tag{7}$$

where $G_E^{Xo}(\mathbf{K})$ is the sum over the relative momentum of the noninteracting two-exciton Green function:

$$G_E^{Xo}(\mathbf{K}) = \frac{1}{L^2} \sum_{\mathbf{k}} \frac{1}{E - \varepsilon^X\left(\frac{\mathbf{K}}{2} + \mathbf{k}\right) - \varepsilon^X\left(\frac{\mathbf{K}}{2} - \mathbf{k}\right)}, \tag{8}$$

where k takes the values $k = 0, \pm 2\pi/L, \pm 4\pi/L, \ldots, \pm\pi/a$.

Formula (7) can be used to relate the parameters g_0 and a of our simple contact interaction model to the actual excitonic T matrix. This T matrix should be determined from a full solution of the two-exciton problem, starting from the Coulomb interactions between the constituent electrons and holes. An accurate calculation of the excitonic T matrix is a highly nontrivial task, and so far calculations based on the Born approximation,[19] the dynamics-controlled truncation scheme,[11,12] and diffusion Monte Carlo calculations[20] are available for excitons in quantum wells.

We will not try to calculate the excitonic T matrix here, but rather investigate its relation to the polaritonic T matrix in the regime of strong exciton-photon coupling. If the

exciton-exciton scattering mainly involves momentum states $\mathbf{k}$ for which the excitonic dispersion $\varepsilon^X(\mathbf{k})$ is quadratic with an effective mass m_X, the center-of-mass (c.m.) and relative motion can be separated. The center-of-mass motion then merely gives a shift of the total energy, and all the information is contained in the $\mathbf{K}=0$ matrix element of Eq. (7). The momenta $\mathbf{k}$ and $\mathbf{k}'$ of interest here will be much smaller than the excitonic interaction range and can be set to zero in Eq. (7), yielding simply

$$\frac{1}{g_0^{\sigma\chi}} = \frac{1}{t_E^{XX,\sigma\chi}} + G_E^{Xo}(0), \tag{9}$$

where $t_E^{XX}=L^{-2}\langle 0,0|T_E|0,0\rangle$, relating together with Eq. (8) explicitly the model parameters $g_0^{\sigma\chi}$ and a to the physical T matrix.

It is worth mentioning in passing that Eqs. (7) and (8) are in fact a justification of the nonlinear term in Eq. (2). The T matrix contains all the information on the two-body physics. For two models to be physically equivalent, it is necessary and sufficient that they reproduce the same T matrix in the relevant energy and momentum ranges. As a bosonic mean-field theory neglects the momentum states different from the condensate momentum, the sum is in Eq. (8) restricted to a single wave vector $k=0$ and it vanishes in the large-area limit $L^2\to\infty$, so that Eq. (2) follows from Eq. (9).

The discussion below Eq. (5) has shown that it is natural to express the coupling constant $t_E^{XX,\sigma\chi}$ as $g^{XX\sigma\chi}=4\pi\hbar^2\eta_E^{\sigma\chi}/m_X$. We now have to make a distinction between the collision of two excitons that are circularly polarized in the same or opposite directions. For cocircular polarization, no biexciton bound state exists so that the T matrix has to be a slowly varying function of the energy (see Ref. 12). Using the theoretical estimate[23] for GaAs, $g^{XX\uparrow\uparrow}=0.015$ meV μm^2, one obtains with $m_X=0.4m_e$ the value $\eta_E^{\uparrow\uparrow}=6$.

For opposite polarizations, on the other hand, the biexcitonic state leads to a resonance in the T matrix. This is easily seen from Eq. (3). A bound biexcitonic state $|b\rangle$ manifests itself as a pole in G_E at the biexcitonic energy E_b. Expanding G_E for $E\approx E_b$,

$$G_E = \tilde{G} + \frac{|b\rangle\langle b|}{E-E_b}, \tag{10}$$

with $|b\rangle$ the biexciton bound state, $t_E^{XX\uparrow\downarrow}$ can be rewritten as

$$t_E^{XX\uparrow\downarrow} \approx t_{\mathrm{nr}}^{XX\uparrow\downarrow} + \frac{4\pi\hbar^2}{m_X}\frac{\Delta}{E-E_b}, \tag{11}$$

where the resonance strength is defined as

$$\Delta = \frac{m_X}{4\pi\hbar^2}|\langle 0,0|V|b\rangle|^2. \tag{12}$$

The resonant structure (11) of the T matrix can also be recognized in Figs. 7 and 8 of Ref. 12. Δ is conveniently rewritten by noting that $\langle 0,0|V|b\rangle=\langle 0,0|\nabla^2/2m_X+V|b\rangle$, thanks to the zero-momentum state in the bra. Using the fact that $|b\rangle$ is a solution of the Schrödinger equation with energy E_b, one obtains

$$\Delta = \frac{m_X(E_b-2\varepsilon^X)^2}{4\pi\hbar^2}|\langle 0,0|b\rangle|^2. \tag{13}$$

In a first approximation, the exciton-exciton interaction can be modeled by a deuteron potential[21] $V(r)=\frac{-27\hbar^2}{4m_Xa^2}e^{-r/a}$, where a satisfies $E_b-2\varepsilon^X=-2\hbar^2/(m_Xa^2)$. A variational calculation with the model relative wave function $\psi(r)=\sqrt{2/\pi\lambda^2}\exp[-r/\lambda]$ yields the lowest energy for $\lambda=a$, so that $\langle 0,0|b\rangle=16\pi/(2\varepsilon_X-E_b)$ and the resonance width equals $\Delta=4(2\varepsilon^X-E_b)$. With the binding energy of a biexciton in GaAs of about 2 meV, we estimate $\Delta\approx 8$ meV, which is large as compared to the excitonic and photonic damping rates and of the same order as the Rabi splitting. This large value of the resonance width Δ is favorable for the experimental observability of the biexcitonic resonance in the polariton-polariton scattering. Because the result $\Delta=4(2\varepsilon^X-E_b)$ is based on a rather crude model of the exciton-exciton interactions, it is instructive to compare with another model calculation. A potential for which the bound state can be calculated exactly is the zero range pseudopotential.[22] The coupling strength Δ equals within this model $\Delta=2\varepsilon^X-E_b$. The fact that it evaluates within the pseudopotential model to a smaller value as compared to the deuteron potential calculation $\Delta=E_b-2\varepsilon^x$ is not unexpected, because in the pseudopotential model, the interactions only take place for zero relative distances. Therefore, the matrix element Δ, which is an overlap of the interaction potential with the bound and scattering wave functions, is smaller. From this reasoning, the pseudopotential calculation is expected to give a lower bound for the value of Δ.

C. Polariton-polariton scattering

Let us now include the exciton-photon coupling in the T matrix. The single-particle eigenstates then form polariton branches, coherent superpositions of excitons and photons. They can be expressed in the exciton-photon basis as

$$|k,J\sigma\rangle = \sum_{\alpha=X,C} H_k^{\alpha J}|k,\alpha\sigma\rangle, \quad J=LP,UP, \tag{14}$$

where the Hopfield coefficients H quantify the excitonic and photonic content of the polariton, whose dispersion will be denoted by $\varepsilon_J(k)$ (see Fig. 1). The T matrix can again be evaluated using the techniques of Ref. 18. The matrix element for two particles in the LP branch is

$$\begin{aligned} g_{\mathbf{Kkk}'}^{\sigma\chi}(E) &= \langle \mathbf{K},\mathbf{k};\sigma\chi|T_E|\mathbf{K},\mathbf{k}';\sigma\chi\rangle_{11} \\ &= \frac{1}{L^2}\frac{H^{X1}_{\mathbf{K}/2+\mathbf{q}}H^{X1}_{\mathbf{K}/2-\mathbf{q}}H^{X1}_{\mathbf{K}/2+\mathbf{q}'}H^{X1}_{\mathbf{K}/2-\mathbf{q}'}}{[T_E]^{-1}-D_E(\mathbf{K})}, \end{aligned} \tag{15}$$

where

$$D_E(\mathbf{K}) = \frac{1}{L^2}\sum_{\mathbf{k},J,J'}\left(\frac{(H^{XJ}_{\mathbf{K}/2+\mathbf{k}})^2(H^{XJ'}_{\mathbf{K}/2-\mathbf{k}})^2}{E-\varepsilon_J(\mathbf{K}/2+\mathbf{k})-\varepsilon_{J'}(\mathbf{K}/2-\mathbf{k})} - \frac{1}{E-\hbar^2k^2/m_X}\right), \tag{16}$$

and Eq. (9) has been used. Because the summation in Eq.

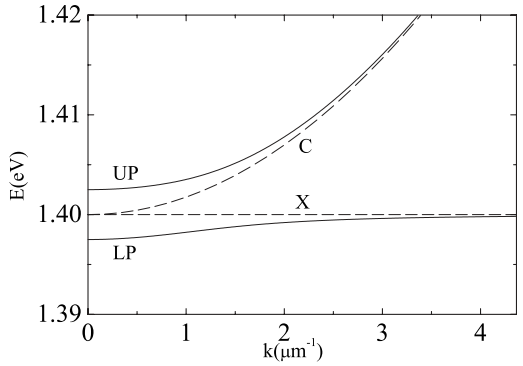

FIG. 1. The dispersions of the uncoupled excitonic (X) and cavity photonic dispersions (C) are shown together with the dispersions of the hybridized lower polariton (LP) and upper polariton (UP). The Rabi frequency was taken $\Omega_R=5$ meV and the cavity frequency $\varepsilon_1^C=1.4$ meV.

(16) converges on the ultraviolet side, we can now safely let the model lattice spacing a tend to zero.

Equations (15) and (16) are central to this paper. They show how the polariton interactions are related to the excitonic ones. The numerator of Eq. (15) contains the usual Hopfield coefficients that take the excitonic content of the polariton into account.[24,25] The term $D_E(\mathbf{K})$ in Eq. (16) is not trivial. It takes into account the renormalization of the interactions due to the fact that also the intermediate states in the scattering process are polaritons instead of pure excitons. Note that, as a consequence of the momentum-independent exciton-exciton interactions in our model Hamiltonian (6), the denominator of Eq. (15) only depends on the c.m. wave vector and not on the relative momenta in the initial and final states. With respect to the model of Ivanov and co-workers,[21] our model is simplified, because the momentum dependence of the excitonic interactions is neglected from the beginning. As argued above, the good separation in the length scales of the strong light-matter coupling physics on the one hand and the excitonic scattering on the other hand ensures that this is a well-controlled approximation.

The effect of the renormalization term is expected to be usually small. The reason can be traced back to the large ratio of the excitonic over the polaritonic mass. From a dimensional analysis, it follows that $D_E(\mathbf{K})=\alpha_E(\mathbf{K})m_{LP}/\hbar^2$, with α_E dimensionless. The summand in Eq. (16) is effectively cut off at wave vectors where the strong exciton-photon coupling is lost, so that it is expected that $\alpha_E(\mathbf{K})$ is of order 1. This is confirmed by numerical calculations. The quantity T_E in Eq. (15) on the other hand is inversely proportional to the excitonic mass [see Eq. (11)]. Therefore, barring excitonic resonances (where t_E^{-1} is small) and "anomalously" large values of $\alpha_E(\mathbf{K})$, the renormalization of the excitonic interactions due to the strong coupling with the cavity photons is negligible.

III. PARAMETRIC INTERACTION STRENGTH CLOSE TO BIPOLARITON RESONANCE

One of the most dramatic effects of interactions in resonantly pumped microcavities is the parametric scattering.[26]

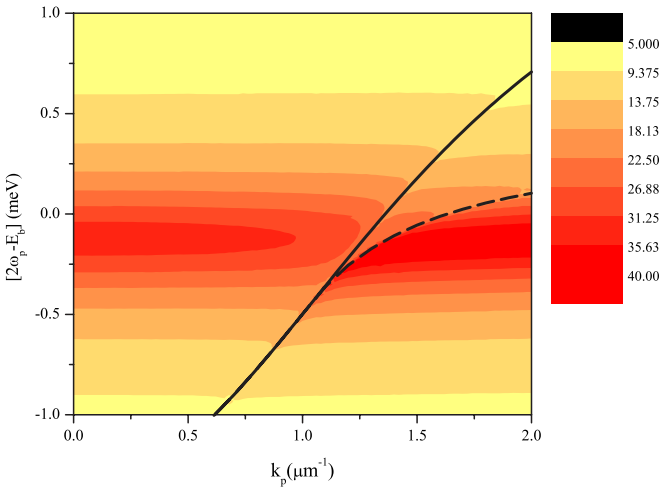

FIG. 2. (Color online) $|t_{2k_p\uparrow\downarrow}(2\omega_p)|$ as a function of the pump angle and pump energy. The solid line shows twice the polariton dispersion $2[\varepsilon(k_p)-\varepsilon(0)]$ and the dashed line shows the maximum in the density of states for $k\neq 0$ (see Fig. 3). The cavity detuning is $\varepsilon^C-\varepsilon^X=2$ meV. The resonance width is taken $\Delta=8$ meV (see text), the background biexciton damping $\Gamma_b=0.2$ meV, and the other cavity parameters are as in Fig. 1.

Two polaritons of the pumped mode with wave vector k_p and frequency ω_p scatter to form a "signal" and "idler" polariton: $2k_p=k_s+k_i$ and $2\omega_p=\omega_s+\omega_i$. As already put forward in Ref. 9, the bipolaritonic scattering resonance can enhance this parametric process. The threshold pump intensity above which the occupation of the modes at k_s and k_i becomes macroscopic is inversely proportional to the modulus of the the coupling constant[27] $|g_{2k_p,k_s,k_p\uparrow\downarrow}(2\omega_p)|$.

Close to the scattering resonance resonance, the background coupling constant t_{bg}^{XX} in Eq. (11) can be neglected. At this point, also loss mechanisms that are not present in our simplified treatment can be included by introducing a phenomenological background line width for the biexciton resonance in Eq. (11): $E_b\rightarrow E_b+i\Gamma_b$.

For a quantitative analysis, we write the coupling constant as $g_{2k_p,k_s,k_p\uparrow\downarrow}=\frac{4\pi\hbar^2}{m_X}H^4t_{2k_p\uparrow\downarrow}$, where H^4 schematically represents the product of four Hopfield coefficients in Eq. (15). Figure 2 shows a plot of $|g_{2k_p,\uparrow\downarrow}(2\omega_p)|$ as a function of the scattering energy $2\omega_p$ and pump wave vector k_p. The solid line shows the free dispersion of two polaritons in the pumped mode. At small k_p, the free polariton dispersion stays far from the biexcitonic state and a strong resonance peak is observed at $E=E_b$, which is almost not shifted with respect to the biexcitonic state. The reason for the weak renormalization is the large ratio of the excitonic mass with respect to the polaritonic one as explained below Eq. (16).

For larger values of k_p, two valleys develop in the the coupling constant $|t_{2k_p\uparrow\downarrow}(2\omega_p)|$. The physical reason is the efficient dissociation of the bipolariton into $k_p\pm k$ pairs. Figure 3 illustrates the scenario. It shows the detuning $E_b-\varepsilon_J(\mathbf{k}_p+k\mathbf{e}_x)-\varepsilon_{J'}(\mathbf{k}_p-k\mathbf{e}_x)$, which is the energy difference between the biexciton state and two outgoing polaritons with c.m. momentum $2\mathbf{k}_p$ and relative momentum k in the x direction. Due to the nonparabolicity of the polariton disper-

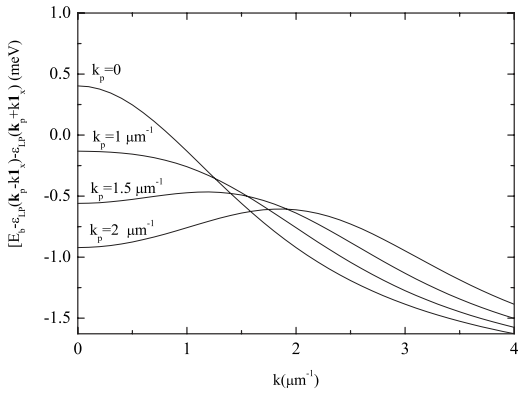

FIG. 3. The detuning between the bipolariton and two free polaritons with c.m. momentum $2k_p$ as a function of their relative momentum in the x direction k for several values of k_p.

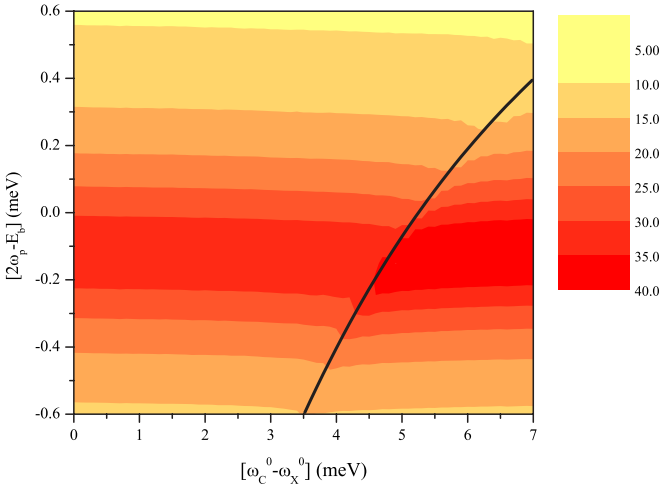

FIG. 4. (Color online) $|t_{2k_p,0,k_s-k_p\uparrow\downarrow}(\omega_p)|$ as a function of the cavity photon-exciton detuning and pump energy. The solid line shows twice the polariton dispersion $2[\varepsilon(0)-E_b]$. The other parameters are the same as in Fig. 2.

sion, this detuning shows a nontrivial dependence on the relative momentum k. Where this function is flat, the density of dissociated states is the largest and their effect on the bipolariton the most pronounced. One maximum is always present at $k=0$, resulting in the logarithmic dependence of the scattering amplitude on the scattering energy close to the free polariton dispersion (see the solid line in Fig. 2). An additional maximum in the density of states develops for sufficiently large k_p and $k\neq 0$. Its location is shown with the dashed line in Fig. 2. Only close to the energy and c.m. wave vector where resonant dissociation of the bipolariton into free polaritons with a large density of states occurs is the renormalization of the scattering amplitude substantial.

From a quantitative point of view, two points are worth discussing. First, Fig. 2 shows that the suppression of the resonance due to the dissociation in free polaritons is not dramatic. For the experimentally realistic parameters that we have used, the maximal value of the coupling constant is for fixed k_p suppressed by a factor of 2 at most. Second, Fig. 2 shows that for the chosen parameters, the dimensionless parametric coupling constant t can become as large as $t\approx 40$. This value of t has to be compared with the typical values $t\approx 6$, estimated for the scattering of cocircular polaritons (see Sec. II B). Our theoretical analysis thus confirms the experimental observation that it is possible to enhance the parametric interactions in the countercircularly polarized channel with respect to the cocircular one by tuning the scattering energy close to the biexcitonic state.[9] Note that the maximal magnitude of the coupling constant depends much on the quality of the sample as it is inversely proportional to the background bipolaritonic lifetime Γ_b.

Such large interactions could raise concern about the validity of mean-field theory, but even though in this form the interactions (for both the cocircularly and countercircularly polarized) polaritons are large ($t>1$), the relevant mass scale to be considered is not the exciton mass m_X, but rather the lower polariton mass $m_{LP}=[d^2\varepsilon_{LP}(k)/dk^2]\approx 10^{-3}m_X$. In the form $g=\frac{4\pi\hbar^2}{m_{LP}}H^4t'$, with $t'=tm_{LP}/m_X\ll 1$, it is apparent that the interactions are actually weak. Because the polariton mass is so much smaller than the excitonic mass, it is in fact extremely difficult to create a strongly interacting polariton gas, in the sense that $t'\gg 1$. This "weak-interaction feature" is directly related to the key advantages of the polaritonic system with respect to the excitonic one: it is also the small polaritonic mass that ensures a large Bose-Einstein condensation temperature[28] ($\propto m_{LP}^{-1}$) and a dominance of the kinetic energy over the disorder potential (motional narrowing[29]).

As a final point, it is also interesting that the resonances in Fig. 2 correspond to the bipolariton, which can be measured alternatively by a four-wave mixing experiment such as, e.g., in Ref. 8. This investigation was restricted to the zero c.m. wave vector of the bipolariton. For comparison with the $k_p\neq 0$ situation, we have also calculated the bipolariton resonance (via the parametric scattering amplitude) for zero c.m. wave vector in Fig. 4. With respect to the finite-k_p case, the renormalization is weaker, because there is only a large density of dissociated states with zero relative wave vector (see Fig. 3 for $k_p=0$). The bipolariton resonance energy is in both Figs. 3 and 4 shifted by about 0.1 meV with respect to the excitonic resonance. This small value of the shift is in qualitative agreement with the experiments of Ref. 8. The experiments of Ref. 6 on the other hand observed a much larger shift of the resonance energy (about 0.6 meV). This could be an indication that the density of polaritons was in the latter experiment too high for a two-particle description of the polariton-polariton interactions to be valid.

IV. SIGNATURES SENSITIVE TO THE SIGN OF THE INTERACTIONS

The above discussion was mainly focused on the strength of the parametric interaction and we have shown how the interactions between countercircularly polarized polaritons can be strongly enhanced by carefully adjusting the cavity detuning, pump angle, and pump energy. The possibility to enhance the interactions is, however, only one feature of a scattering resonance. In an OPO experiment, the scattering resonance then leads to a decrease of the threshold, but due

to the complicated phenomenology of the OPO process itself (see, e.g., Ref. 27), other experimental investigations are necessary for a clear understanding of the scattering resonance. We propose two such alternatives in the present section: the mean-field shifts and the direction of the linear polarization of parametric luminescence below the threshold. These quantities are sensitive to the sign of the interactions between the countercircularly polarized polaritons, which can be varied by crossing the resonance.[30]

A. Mean-field shifts

In a cavity pumped with circularly ↑-polarized resonant laser light, the density of polaritons in the pump mode n_p shifts the single-polariton dispersion.[24] The direction of the shift of the spin-down polaritons depends on the sign of $g_{\uparrow\downarrow}$. Equations (11) and (15) show that the sign of the interactions close to the resonance is positive (repulsive) for scattering energies above the bi-polariton state, whereas they are negative (attractive) for scattering energies below the resonance. The dispersion of the polaritons can be experimentally determined from transmission measurements with a weak counterpolarized probe beam such as, e.g., in Ref. 6.

The theoretical prediction for the ↓-polarized probe transmittivity is in linear response theory

$$T(k,E) \propto \frac{1}{|E-[\varepsilon(k)-i\gamma/2+g_{k_p+k,k-k_p,k-k_p\uparrow\downarrow}(\omega_p+E)n_p]|}, \tag{17}$$

where γ is the width of the polariton luminescence at the linear regime. The prediction (17) for the transmittivity is plotted in Fig. 5 for a microcavity resonantly pumped at $k=1\ \mu\mathrm{m}^{-1}$ (below the magic angle to avoid parametric oscillation).

The mean-field shift of a polariton with energy higher (lower) than the bipolariton is positive (negative), giving rise to the upper (lower) branch of luminescence. For the luminescence wave vectors k where the polariton dispersion is close to the bipolariton resonance, both branches of luminescence are present. The peculiar behavior of the mean-field shifts shown in Fig. 5 can be seen as a fingerprint of the resonance. Its shape can be easily understood. A polariton with a wave vector that is close to satisfy the resonance condition $\epsilon(\mathbf{k})+\epsilon(\mathbf{k}_p)=E_b$ is shifted upwards when its energy is larger than $E_b-\omega_p$, leading self-consistently to a maximum above the bare polariton branch. It is on the other hand shifted downwards when its energy is below $E_b-\omega_p$, so that also a self-consistent maximum of the luminescence below the bare polariton branch exists.

The proposed configuration where the biexciton energy is higher than the bottom of the lower polariton branch should be more favorable to probe the resonant behavior of mean-field shifts as compared to the configuration of Ref. 6 where the biexciton resonance was below the minimum of the lower polariton branch and only a blueshift was observed.

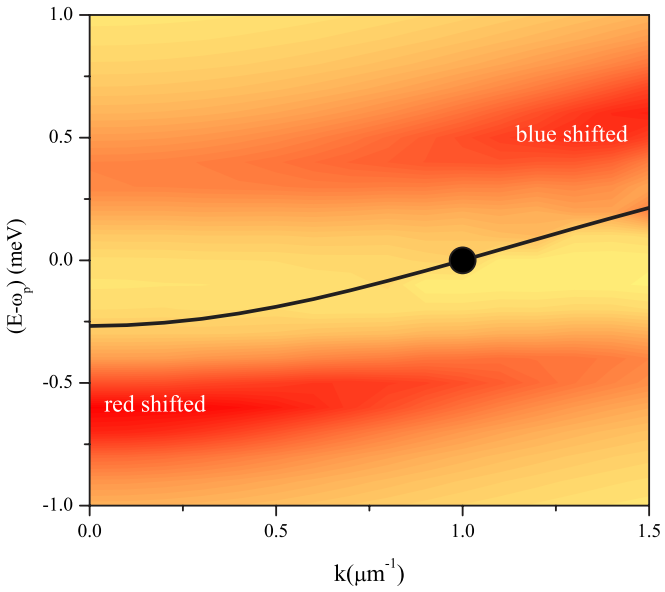

FIG. 5. (Color online) The spin ↓-probe transmittivity of the microcavity as a function of the wave vector and energy, for a ↑-pump polariton density of $2\times10^8\ \mathrm{cm}^{-2}$, and a resonant pump laser at $k_p=1\ \mu\mathrm{m}^{-1}$ (shown with a black circle). For low (high) wave vectors, the mean-field shifts are in the red (blue) direction. The polariton linewidth is taken to be $\gamma=0.2$ meV. The polariton dispersion in the absence of the pump is shown with a black line.

B. Orientation of the linear polarization of parametric luminescence

A second way to study the sign change of the interactions is to analyze the polarization properties of the parametric emission. The discussion in Sec. III focused on the modulus of the interactions, and the relation to the threshold of parametric oscillation was pointed out. A microcavity pumped with linearly polarized light below the threshold for OPO shows a linear polarization of the signal emission that is[31] (i) aligned with the linear polarization of the pump light if $\mathrm{Re}[g^{\uparrow\uparrow}g^{\uparrow\downarrow}]>0$ and (ii) rotated by 90° with respect to the linear polarization of the pump light if $\mathrm{Re}[g^{\uparrow\uparrow}g^{\uparrow\downarrow}]<0$. Because $g^{\uparrow\uparrow}$ is shown to be positive, the measurement of the polarization directly gives information on the sign of $g^{\uparrow\downarrow}$. By varying the detuning, it is possible to have the energy of two pump polaritons both above and below the bipolariton energy so that both orientations can be observed, again serving as a clear signature of the scattering resonance. In addition, the possibility to change the polarization direction of the parametric emission could have technological applications in the framework of spin-dependent optoelectronic devices.[34]

V. CONCLUSIONS

We have studied the interactions between polaritons in microcavities and their renormalization due to strong light-matter coupling. A distinction has to be made between cocircularly and countercircularly polarized polaritons. In the first configuration, the polaritonic interactions are simply related to the excitonic ones via the Hopfield coefficients, whereas

in the second configuration, nontrivial renormalization effects take place close to the bipolariton scattering resonance. The width of the resonance was estimated within a deuteron potential approach for the exciton-exciton interactions, and it was shown that, taking a realistic width for the bipolariton, the polaritonic interaction strength in the $\uparrow\downarrow$ channel can become larger than the one in the $\uparrow\uparrow$ channel. The energy dependence of the parametric scattering was analyzed, and the resonant dissociation of the bipolariton into free polaritons with a large density of states was shown to suppress the interaction strength.

We have also shown that the mean-field shifts have a particular energy and wave vector dependence, with both redshifts and blueshifts, which serve as a fingerprint for the bipolaritonic resonance. In addition, it was pointed out that the linear polarization orientation of the parametric luminescence can be changed by making use of the scattering resonance.

ACKNOWLEDGMENTS

Fruitful discussions with G. C. La Rocca and H. Zoubi on polariton interactions and continuous stimulating discussions with I. Carusotto, J. Tempere, and J. T. Devreese are gratefully acknowledged. This research has been supported financially by FWO-V Projects Nos. G.0435.03, G.0115.06, the Special Research Fund of the University of Antwerp, BOF NOI UA 2004, and the FWO-Vlaanderen in the form of a "mandaat Postdoctoraal Onderzoeker."

[1] S. Inouye *et al.*, Nature (London) **392**, 6672 (1998).
[2] A. J. Moerdijk, H. M. J. M. Boesten, and B. J. Verhaar, Phys. Rev. A **53**, 916 (1996).
[3] E. A. Donley *et al.*, Nature (London) **412**, 295 (2001).
[4] C. A. Regal, M. Greiner, and D. S. Jin, Phys. Rev. Lett. **92**, 040403 (2004); M. W. Zwierlein, C. A. Stan, C. H. Schunck, S. M. F. Raupach, A. J. Kerman, and W. Ketterle, *ibid.* **92**, 120403 (2004); C. Chin *et al.*, Science **305**, 1128 (2004); T. Bourdel, L. Khaykovich, J. Cubizolles, J. Zhang, F. Chevy, M. Teichmann, L. Tarruell, S. J. J. M. F. Kokkelman, and C. Salomon, Phys. Rev. Lett. **93**, 050401 (2004); J. Kinast *et al.*, Science **307**, 1296 (2005).
[5] R. M. Stevenson, V. N. Astratov, M. S. Skolnick, D. M. Whittaker, M. Emam-Ismail, A. I. Tartakovskii, P. G. Savvidis, J. J. Baumberg, and J. S. Roberts, Phys. Rev. Lett. **85**, 3680 (2000); R. Houdre, C. Weisbuch, R. P. Stanley, U. Oesterle, and M. Ilegems, *ibid.* **85**, 2793 (2000).
[6] M. Saba, F. Quochi, C. Ciuti, U. Oesterle, J. L. Staehli, B. Deveaud, G. Bongiovanni, and A. Mura, Phys. Rev. Lett. **85**, 385 (2000).
[7] S. Adachi, T. Miyashita, S. Takeyama, T. Takagi, A. Tackeuchi, and M. Nakayama, Phys. Rev. B **55**, 1654 (1997); T. Tsuchiya, Phys. Status Solidi C **1**, 603 (2004).
[8] A. L. Ivanov, P. Borri, W. Langbein, and U. Woggon, Phys. Rev. B **69**, 075312 (2004).
[9] A. I. Tartakovskii, D. N. Krizhanovskii, and V. D. Kulakovskii, Phys. Rev. B **62**, R13298 (2000); D. N. Krizhanovskii *et al.*, Phys. Status Solidi A **202**, 2621 (2005).
[10] P. G. Lagoudakis, P. G. Savvidis, J. J. Baumberg, D. M. Whittaker, P. R. Eastham, M. S. Skolnick, and J. S. Roberts, Phys. Rev. B **65**, 161310(R) (2002).
[11] N. H. Kwong, R. Takayama, I. Rumyantsev, M. Kuwata-Gonokami, and R. Binder, Phys. Rev. Lett. **87**, 027402 (2001); Phys. Rev. B **64**, 045316 (2001).
[12] R. Takayama, N. H. Kwong, I. Rumyantsev, M. Kuwata-Gonokami, and R. Binder, Eur. Phys. J. B **25**, 445 (2002).
[13] S. K. Adhikari, Am. J. Phys. **54**, 362 (1986).
[14] D. S. Petrov and G. V. Shlyapnikov, Phys. Rev. A **64**, 012706 (2001).
[15] M. Schick, Phys. Rev. A **3**, 1067 (1971).
[16] S. Cowell, H. Heiselberg, I. E. Mazets, J. Morales, V. R. Pandharipande, and C. Pethick, Phys. Rev. Lett. **88**, 210403 (2002).
[17] M. Z. Maialle, E. A. de Andrada e Silva, and L. J. Sham, Phys. Rev. B **47**, 15776 (1993).
[18] Y. Castin, J. Phys. IV **116**, 89 (2004).
[19] C. Ciuti, V. Savona, C. Piermarocchi, A. Quattropani, and P. Schwendimann, Phys. Rev. B **58**, 7926 (1998).
[20] J. Shumway, Physica E (Amsterdam) **32**, 273 (2006).
[21] A. L. Ivanov, H. Haug, and L. V. Keldysh, Phys. Rep. **296**, 237 (1998).
[22] E. Fermi, Ric. Sci. **7**, 13 (1936); K. Huang and C. N. Yang, Phys. Rev. **105**, 767 (1957); K. Wódkiewicz, Phys. Rev. A **43**, 68 (1991).
[23] A. Verger, C. Ciuti, and I. Carusotto, Phys. Rev. B **73**, 193306 (2006).
[24] C. Ciuti, P. Schwendimann, B. Deveaud, and A. Quattropani, Phys. Rev. B **62**, R4825 (2000).
[25] D. M. Whittaker, Phys. Rev. B **63**, 193305 (2001).
[26] P. G. Savvidis, J. J. Baumberg, R. M. Stevenson, M. S. Skolnick, D. M. Whittaker, and J. S. Robe, Phys. Rev. Lett. **84**, 1547 (2000); R. M. Stevenson, V. N. Astratov, M. S. Skolnick, D. M. Whittaker, M. Emam-Ismail, A. I. Tartakovskii, P. G. Savvidis, J. J. Baumberg, and J. S. Roberts, *ibid.* **85**, 3680 (2000); R. Houdré, C. Weisbuch, R. P. Stanley, U. Oesterle, and M. Ilegems, *ibid.* **85**, 2793 (2000); J. J. Baumberg, P. G. Savvidis, R. M. Stevenson, A. I. Tartakovskii, M. S. Skolnick, D. M. Whittaker, and J. S. Roberts, Phys. Rev. B **62**, R16247 (2000); C. Ciuti, P. Schwendimann, and A. Quattropani, *ibid.* **63**, 041303 (2001); D. M. Whittaker, *ibid.* **63**, 193305 (2001).
[27] M. Wouters and I. Carusotto, Phys. Rev. B **75**, 075332 (2007).
[28] J. Kasprzak *et al.*, Nature (London) **443**, 409 (2006).
[29] D. M. Whittaker, Phys. Rev. Lett. **80**, 4791 (1998).
[30] An analogous sign change was used in the Bose nova experiments with ultracold atoms of Doneley *et al.* (Ref. 3), where the sign of the interactions in a BEC was rapidly changed from positive to negative. This resulted in a collapse of the BEC and a subsequent explosion. An analogous implosion of the resonantly pumped microcavity system is not to be expected when the interactions between the polaritons are attractive, because the instability with respect to the implosion of the system is of ener-

getic nature. Since the resonantly pumped microcavity system is far from thermodynamical equilibrium anyway (the polaritons are mostly in the pumped high-energy state and not close to the bottom of the dispersion), energetic instabilities are not expected to play an important role.

[31] K. V. Kavokin *et al.*, Phys. Status Solidi C **2**, 763 (2005). Reference 32 gives a general discussion of spin dynamics in microcavities. An experimental study and refinement of the rotation by 90° is presented in Ref. 33.

[32] I. A. Shelyk, A. V. Kavokin, and G. Malpuech, Phys. Status Solidi A **242**, 271 (2005).

[33] D. N. Krizhanovskii, D. Sanvitto, I. A. Shelykh, M. M. Glazov, G. Malpuech, D. D. Solnyshk, A. Kavokin, S. Ceccarelli, M. S. Skolnick, and J. S. Roberts, Phys. Rev. B **73**, 073303 (2006).

[34] I. Shelykh, K. V. Kavokin, A. V. Kavokin, G. Malpuech, P. Bigenwald, H. Deng, G. Weih, and Y. Yamamoto, Phys. Rev. B **70**, 035320 (2004).